Average PSNR Optimized Cross Layer User Grouping and Resource Allocation for Uplink MU-MIMO OFDMA Video Communications

SHU-MING TSENG[ID]**[1], (Member, IEEE), AND YUNG-FANG CHEN**[ID]**[2], (Member, IEEE)**

[1]Department of Electronic Engineering, National Taipei University of Technology, Taipei 106, Taiwan
[2]Department of Communication Engineering, National Central University, Taoyuan 320, Taiwan

Corresponding author: Shu-Ming Tseng (shuming@ntut.edu.tw)

ABSTRACT Wang *et al.* proposed cross layer resource allocation according to the channel state information of the physical layer and the video rate distortion of the application layer for uplink orthogonal frequency division multiple access (OFDMA) video transmission systems. Its object function is minimizing sum of all users' video distortion. It shows significant improvement in average peak-signal-to-noise-ratio (PSNR) over the schemes which consider either the physical layer or application layer. However, minimizing sum of all users' video distortion does not necessarily maximize average of all users' PSNR. In this paper, we change the objective function for optimization to maximize average PSNR, and derive new optimal condition for cross layer subcarrier assignment for infinitesimal bandwidth increment. Furthermore, we extend to a multi-user multiple-input and multiple-output (MU-MIMO) uplink transmission system to improve information rate and thus video quality. We then propose an average PSNR optimized physical/application cross-layer user grouping and resource allocation for uplink MU-MIMO OFDMA video communications. The simulation results show that the proposed scheme has 4 dB PSNR gain over the previous Wang *et al.* cross-layer scheme and 5 dB PSNR gain over the previous physical layer only scheme for four users and SNR 12–18 dB.

INDEX TERMS Sum PSNR maximization, sum distortion minimization, multi user multiple input multiple output (MU-MIMO), user grouping, peak-signal-to-noise-ratio (PSNR), video communications.

I. INTRODUCTION

Orthogonal Frequency Division Multiple Access (OFDMA) is the transmission technology of many wireless communication systems including DVB-T2, WiMAX and LTE [1]–[6] due to its high spectrum efficiency, resistance to delay spread, and flexible resource allocation. The resource allocation according to user's service requirements is a crucial topic in OFDMA systems. Like [7]–[9], it often considers the channel state information (CSI) in the physical layer for assigning the resources. With imperfect CSI, resource assignment is considered in [7] and [8]. In [9], the resource allocation is to optimize the weighted sum of user coding gaps when weight factor denotes the importance level of users. In addition to using the physical layer, the resource allocation in [10]–[17] is based on the rate distortion (RD) information in the application layer. In [10] and [11], different video RD functions provide a chance to improve total video quality. In [12], bit rate allocation utilizes the competitive

equilibrium. In [13], a video is divided into video layers by scalable video coding and user fairness is considered in the resource allocation. In [14], fairness and efficiency trade-off is considered. In [15] and [16], fairness and efficiency are considered for resource allocation crossing the medium access control (MAC) layer and application layer. In [17], un-coded multi-user video transmissions result in closed-form video distortion, and comparison is made among different optimization objective: minimization of total distortion, maximum distortion, or summation of square root distortion. To be better than using either the physical or application layer, [18] gives a physical/application cross layer resource allocation which combines RD information (application layer) and CSI (physical layer) to minimize the sum of the users' video distortion (mean square error, MSE) for uplink OFDMA video communication systems. Reference [19] extends [18] to include Hybrid Automatic Repeat reQuest (HARQ) and turbo code and improve video quality at the cost of

extra delay. Reference [20] extends further for anti-jamming scenarios. However, [18]–[20] have only one user on each subcarrier and do not consider Multi-User Multiple-Input and Multiple-Output (MU-MIMO) for substantial information rate increase and thus video quality improvement. Furthermore, they minimize the sum video distortion and do not directly maximize the average Peak-Signal-to-Noise-Ratio (PSNR), the video quality.

MU-MIMO allows a base station (BS) and multiple single-antenna users to communicate with each other using the same time slot-subcarrier resource [6], [21]. The resource allocation in transmission rate, subcarrier, transmitter power, user selection etc. improves the system performance such as the sum rate [22]–[29]. The downlink case is considered in [22]–[26]. References [23] and [24] consider allocating subcarriers, rate, and power to the different users in MU-MIMO downlink OFDMA systems. Reference [25] proposes a cluster-based resource allocation in multi-cell scenario of MU-MIMO downlink OFDMA systems. In [26], a resource allocation considering different user's frame size is proposed for downlink MU-MIMO OFDMA systems. Reference [22] is an overview about the resource allocation for downlink MU-MIMO systems. The uplink case is considered in [27]–[29]. Reference [27] proposes the resource allocation algorithm involving user selection, BS selection, and resource block selection for uplink multi-cell MU-MIMO systems. Reference [28] proposes the resource allocation maximizing the energy efficiency, which is more important in the uplink. In [29], the ZF-SVD physical layer resource allocation assumes that the zero-forcing (ZF) post-processing using all users' CSI is at the BS and singular value decomposition (SVD) pre-processing using local CSI is at the MS. The resource allocation of the above references, however, do not cross the application layer. In other words, they don't consider each user's video content's different RD information.

In this paper, we propose a novel resource allocation algorithm crossing the physical and the application layers for uplink MU-MIMO OFDMA video systems. This resource allocation algorithm maximize the video quality, average PSNR, and considers user grouping, subcarrier assignment, rate allocation, and transmitter power assignment. The novelty and contribution of this paper are:

1) Average PSNR is the measure for video quality but [18]–[20] minimize the sum of the users' video distortion (mean square error, MSE) and not maximize the average PSNR directly. We change the optimization objective function to maximize average PSNR (equivalent to minimize the product of the users' MSE) and derive a new optimal condition for infinitesimal bandwidth increment. In the numerical results, this change contributes 2dB gain in PSNR (Scheme B over Scheme A in Figs 3-5)

2) We add MU-MIMO to improve PSNR further and consider extra user grouping problem in the cross layer resource allocation. For initial subcarrier assignment/user grouping, we propose to select the

user group with smallest sum of the noise enhancement factors after zero-forcing MU-MIMO detector (defined in (2) and (13)) among all possible user pairs on each subcarrier. For subcarrier reassignment, user grouping cases are considered on each candidate subcarrier, the products of the users' MSEs which includes the noise enhancement factor are computed. After subcarrier reassignment, different user group occupies this subcarrier. For comparison, [18]–[20] are not MU-MIMO systems, so they don't consider user grouping problem. In the numerical results, this change contributes further 2dB gain in PSNR (Scheme C over Scheme B in Figs. 3-5).

3) Motivated by the new optimal condition in 1), we propose a new iterative physical/application cross layer subcarrier assignment/user grouping scheme. We give priority of gaining a subcarrier to the user who has the largest absolute value of RD curve slope divided by its MSE. If a subcarrier reassignment provides smaller product of the users' MSE, we perform the subcarrier reassignment. For comparison, [18]–[20] give the user with largest absolute value of RD curve slope (not divided by MSE) priority to gain subcarriers and the subcarrier reassignment is evaluated by smaller sum (not product) of the users' MSE.

The rest of this paper is organized as follows: Sec. II introduces the system model. We give a new optimal condition maximizing average PSNR for infinitesimal bandwidth increment in Sec. III. We then propose an iterative cross layer resource allocation for MU-MIMO OFDMA video transmission systems in Sec. IV. The numerical results are shown in Sec. V. The conclusion is given in Sec. VI

II. SYSTEM MODEL
A. OFDMA SYSTEM MODEL

We show the block diagram of the uplink OFDMA system in Fig. 1. The system model is similar to that in [18] except for two blocks in gray. One block is MU-MIMO resource allocation. The other one is FFT, zero forcing MU-MIMO detector, and P/S. The uplink OFDMA video communication system has K users and the user index $k = \{1, 2, \ldots K\}$. The bandwidth W is equally split into M subcarriers, so the bandwidth of one subcarrier is $dw = W/M$. The subcarrier index is $m = \{1, 2, \ldots M\}$. The same as [18], we assume the system operates in a slotted manner. The resource allocation is conducted once for each slot.

B. ZERO FORCING MU-MIMO DETECTOR

Fig. 2 is a $[1, 1] \times 2$ OFDM MU-MIMO system model for users k and l sharing the same subcarrier m, where $k, l = \{1, 2, 3 \ldots K\}$, and $k \neq l$. $[1, 1] \times 2$ means that there are two single-antenna users at the transmitter and one BS with two receive antennas at the receiver. The received vector on
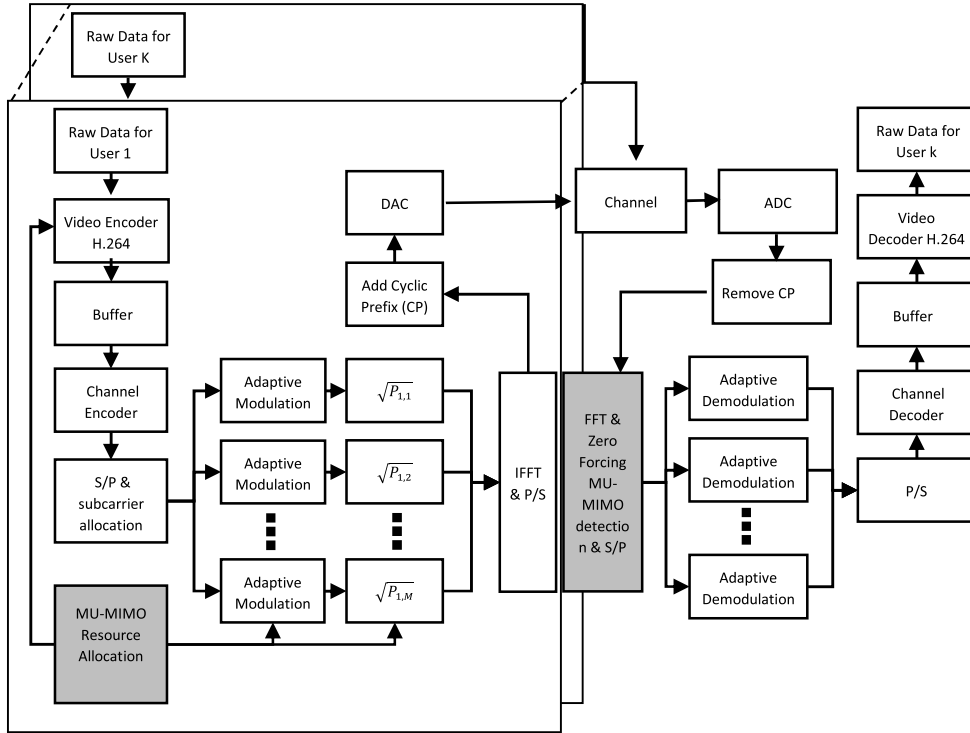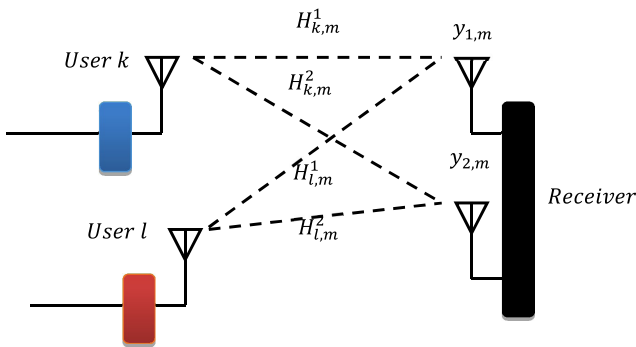
FIGURE 1. The proposed system block diagram.

FIGURE 2. [1, 1] × 2 MU-MIMO for users k and l on subcarrier m.

subcarrier m can be written as

$$\begin{bmatrix} y_m^1 \\ y_m^2 \end{bmatrix} = \begin{bmatrix} H_{k,m}^1 & H_{l,m}^1 \\ H_{k,m}^2 & H_{l,m}^2 \end{bmatrix} \begin{bmatrix} x_{k,m} \\ x_{l,m} \end{bmatrix} + \boldsymbol{n}_m$$

$$= \begin{bmatrix} \boldsymbol{H}_{k,m} & \boldsymbol{H}_{l,m} \end{bmatrix} \begin{bmatrix} x_{k,m} \\ x_{l,m} \end{bmatrix} + \boldsymbol{n}_m = \boldsymbol{H}_m \boldsymbol{x}_m + \boldsymbol{n}_m,$$

(1)

$\begin{bmatrix} y_m^1 \\ y_m^2 \end{bmatrix}$ is the receiver signal vector at two receive antennas (superscript 1 and 2); $\boldsymbol{x}_m = \begin{bmatrix} x_{k,m} \\ x_{l,m} \end{bmatrix}$ is the transmitted symbol vector. $\boldsymbol{H}_{k,m} = \begin{bmatrix} H_{k,m}^1 \\ H_{k,m}^2 \end{bmatrix}$ is the Rayleigh fading channel vector from user k to two receive antennas (superscript 1 and 2)

on subcarrier m. $\boldsymbol{H}_{l,m} = \begin{bmatrix} H_{l,m}^1 \\ H_{l,m}^2 \end{bmatrix}$ is the Rayleigh fading channel vector from user l to two receive antennas (superscript 1 and 2) on subcarrier m. $\boldsymbol{H}_m = \begin{bmatrix} \boldsymbol{H}_{k,m} & \boldsymbol{H}_{l,m} \end{bmatrix}$ is the MU-MIMO Rayleigh fading channel matrix on subcarrier m.

To detect $\boldsymbol{x}_m$, we need to find a matrix $\boldsymbol{W}_m$ which satisfies $\boldsymbol{W}_m \boldsymbol{H}_m = \boldsymbol{I}$. The Zero Forcing (ZF) MU-MIMO detector for meeting this constraint is given by [30]

$$\boldsymbol{W}_m = \left(\boldsymbol{H}_m^H \boldsymbol{H}_m \right)^{-1} \boldsymbol{H}_m^H = \begin{bmatrix} w_{1,m}^1 & w_{2,m}^1 \\ w_{1,m}^2 & w_{2,m}^2 \end{bmatrix}$$

The noise enhancement factor vector for user k and user l is defined as

$$\begin{bmatrix} z_{k,l,m} \\ z_{l,k,m} \end{bmatrix} = \begin{bmatrix} \left(w_{1,m}^1 \right)^2 + \left(w_{2,m}^1 \right)^2 \\ \left(w_{1,m}^2 \right)^2 + \left(w_{2,m}^2 \right)^2 \end{bmatrix}$$

(2)

C. VIDEO MSE DISTORTION

The model of the video MSE distortion is similar to that in [18] except for the equivalent channel response $\left| H_{k,m} \right|^2$ due to two receive antennas and additional parameter $z_{k,m}$ due to ZF MU-MIMO detector. The information rate for user k, subcarrier m (in bits/sec) is

$$R_{k,m} \left(P_{k,m}, H_{k,m}, z_{k,l,m}, P_{l,m}, H_{l,m} \right)$$

$$= dw * min \left\{ \log_2 \left[1 + \eta P_{k,m} \overline{\left| H_{k,m} \right|^2} / z_{k,l,m} \right], R_{max} \right\}$$

(3)

where dw is the bandwidth of one subcarrier defined in Sec. IIA, $P_{k,m}$ is the allocated power for user k on

subcarrier m. $\overline{|H_{k,m}|^2} = \frac{1}{2}\sum_{n=1}^{2}|H_{k,m}^n|^2$ is the equivalent channel response for user k on subcarrier m. $\eta = \frac{3}{P_N}[Q^{-1}(SER_t/4)]^{-2}$ [18], SER_t is the target symbol error rate. The noise power after ZF MU-MIMO detector is the noise power P_N multiplied by $z_{k,m}$. R_{max} denotes the maximum modulation size. Define MSE_k as the user k's rate distortion function, and it is given by [31].

$$MSE_k = a_k + \frac{\omega_k}{B_k + \upsilon_k} \qquad (4)$$

where a_k, ω_k and υ_k depend on the video content. The encoder generates B_k bits:

$$\sum_{m=1}^{M} B_k = u \cdot R_{k,m}\left(P_{k,m}, H_{k,m}, z_{k,l,m}, P_{l,m}, H_{l,m}\right) \cdot T_s/T_0 \qquad (5)$$

A fixed rate u channel code is added to protect the data. The time slot length is T_s(sec). T_0 is the duration of an OFDM symbol. If we combine (5) and (4), the MSE distortion for user k is

$$MSE_k = a_k + \frac{b_k}{\sum_{m=1}^{M} R_{k,m}\left(P_{k,m}, H_{k,m}, z_{k,l,m}, P_{l,m}, H_{l,m}\right) + c_k} \qquad (6)$$

where $b_k = \frac{\omega_k}{(u \cdot T_s/T_0)}$, and $c_k = \frac{\upsilon_k}{(u \cdot T_s/T_0)}$.

When the video is in slow motion and picture is spatially uniform, b_k is relatively small and the RD function is relatively flat. On the contrary, when the video has less time and spatial redundancy, b_k is relatively large and the RD function is relatively steep. The physical/application cross layer resource allocation algorithm exploits the application layer diversity where different users have different RD tradeoff.

D. AVERAGE PSNR OPTIMIZATION
In the uplink OFDMA video communication system, we want to maximize the average PSNR. The PSNR for user k is $10log_{10}\frac{255*255}{MSE_k}$ [18]. Thus the average PSNR is given by

$$\frac{1}{K}\sum_{k-1}^{K} 10log_{10}\frac{255*255}{MSE_k}$$
$$= 10log_{10}(255*255) - \frac{1}{K}\sum_{k-1}^{K}10log_{10}MSE_k \quad (7)$$

To maximize the average PSNR is equal to minimize the product of all users' video distortion. In other words,

$$\min_{\underline{P}} \prod_{k=1}^{K} MSE_k, \qquad (8)$$

where $\underline{P}$ is the power assignment matrix whose (k, m) entry $P_{k,m}$ is the allocated power for user k on subcarrier m. Each uplink user has the same power budget P over all subcarriers, and every subcarrier is shared by two users by MU- MIMO. Thus the average PSNR optimization in (8) has the following constraints:

C1: $\sum_{m=1}^{M} P_{k,m} = P$ *for all 'k*

C2: For $m \in \{1, 2, \ldots, M\}$, $S_m = \{k'|P_{k',m} \neq 0\}$, $\|S_m\| = 1$ or 2, where $\|S_m\|$ denotes the cardinality of the set S_m. That is, at most two users occupy subcarrier m.

Note that C2 is not convex, the average PSNR optimization in (8) is NP-hard. We then propose a suboptimal algorithm. Before describing it in Sec. IV, we first study the optimization condition for the case of the infinitesimal bandwidth increment, as compared to that the bandwidth of a single subcarrier is the minimum bandwidth increment in the OFDMA system. We gain insights from the optimal condition and the proposed algorithm in Sec. IV is thus motivated.

III. AVERAGE PSNR MAXIMIZED OPTIMAL CONDITION FOR INFINITESIMAL BANDWIDTH INCREMENT
Unlike in [18], we consider to maximize the average (or sum) PSNR directly, and not to minimize the sum distortion.

We consider that the frequency channel response is continuous (and thus the infinitesimal bandwidth increment) and there are only two users. User i is assigned the frequency band B_i, and has the channel response $H_i(f)$. The optimization problem is given by

$$\min_{\underline{P}} \prod_{i=1}^{2}\left(a_i + \frac{b_i}{\int_{\hat{B}_k} \log_2[1 + \eta P_i(f)|H_i(f)|^2/z_i]df + c_i}\right) \quad (9)$$

We define the following which will be used in Theorem I.
Definition I:

a) $|.|$ denotes the bandwidth. For example. $\left|B_i^{opt}\right|$ is the bandwidth in Hz of B_i^{opt}, user i's optimal band assignment.

b) z_i is the noise enhancement factor after ZF MU-MIMO detector for user i. z_i is considered as constant for any frequency assignment, i.e. it does not depend on frequency and the 'companion user' sharing the frequency with user i in multiuser mode does not change.

c) $r_i = \int_{B_i^{opt}} \log_2(1 + \eta P_i(f)|H_i(f)|^2/z_i)df$ is the optimal information rate for user $i = 1, 2$.

d) $W_i = P_i(f) + \frac{1}{\eta|H_i(f)|^2/z_i}$ is the optimal water-filling level for user $i = 1, 2$

e) $\theta \in B_2^{opt}$ is an infinitesimal band for user 2, H_i^θ is the channel response in band θ for user $i = 1, 2$,

f) $\varphi_i^\theta = \left(W_i - \frac{1}{\eta|H_i^\theta|^2}\right)^+$ is the non-negative difference between the noise level and water-filling level for user $i = 1, 2$ at band θ, where $[x]^+ = x$ if x > 0, and $[x]^+ = 0$ if x $\leq$ 0.

Theorem 1: For a continuous frequency band B^{tot}, the optimal frequency band assignment B_1^{opt} and B_2^{opt} minimize the average PSNR, and it should satisfy the following for any band θ.

$$\frac{\frac{b_1}{MSE_1(r_1+c_1)^2}\left\{\ln\left(1+\eta\phi_1^\theta\left|H_1^\theta\right|^2\right)-\int_{B_1^{opt}}\frac{\eta|H_1(f)|^2/z_1}{\left|B_1^{opt}\right|(1+\eta P_1(f)|H_1(f)|^2/z_1)}\phi_1^\theta\,df\right\}}{\frac{b_2}{MSE_2(r_2+c_2)^2}\left\{\ln\left(1+\eta\phi_2^\theta\left|H_2^\theta\right|^2\right)-\int_{B_2^{opt}}\frac{\eta|H_2(f)|^2/z_2}{\left|B_2^{opt}\right|(1+\eta P_2(f)|H_2(f)|^2/z_2)}\phi_2^\theta\,df\right\}}\leq 1 \qquad (10)$$

Proof: Please see Appendix A.

$$APP_i = \frac{b_i}{MSE_i\,(r_i+c_i)^2} \qquad (11)$$

$$PHY_i = \left\{\begin{array}{l}\ln\left(1+\eta\phi_i^\theta\left|H_i^\theta\right|\right)\\[2em]-\int_{B_i^{opt}}\frac{\eta\,|H_i(f)|^2/z_i}{\left|B_i^{opt}\right|(1+\eta P_i(f)\,|H_i(f)|^2/z_i)}\phi_i^\theta\,df\end{array}\right\} \qquad (12)$$

The numerator and denominator of (10), as shown at the top of this page, is the product of (11) and (12), for $i=1,2$, respectively. (11) is the absolute value of the RD curve slope $\left(\frac{b_i}{(r_i+c_i)^2}\right)$ divided by MSE_i in layer 5 and functions as a weighting, and (12) is layer 1 information. The insight from (11) is that the user with the steepest RD function slope divided by MSE_i has priority to gain subcarriers. From (12), as $|\theta|$ becomes infinitesimal, (12) is the marginal rate change when a user gains band θ from another user. The first part of (12) is the layer 1 rate variation due to the assignment of θ. The second part of (12) is layer 1 rate variation due to the water-filling level variation and the noise enhancement factor z_i for user i.

From the above analysis, the insights are summarized as follows:

- From (11), the candidate to gain subcarriers is the user with the largest APP_i, which is $\frac{b_i}{(r_i+c_i)^2}$, absolute value of RD function slope, divided by MSE_i (largest weighting). For comparison, the weighting is $\frac{b_i}{(r_i+c_i)^2}$ in [18].
- (12) is the marginal rate change when a user gains band θ from another user. The effect of MU-MIMO is shown in (12) in terms of the noise enhancement factor z_i.
- The physical/application cross layer resource assignment scheme should allocate the frequency band θ to the user with maximum product of (11) (layer 5) and (12) (layer 1).

So far, the bandwidth increment was infinitesimal. However, whereas in the OFDMA systems, the increment is one subcarrier's bandwidth. Thus, the physical layer metric in (12) is no longer valid. We then design an iterative resource allocation algorithm in the following section. Motivated by the optimal condition in (10), the user with largest

$APP_i = \frac{b_i}{MSE_i(r_i+c_i)^2}$ has the priority to win over subcarriers from another user.

IV. PROPOSED MU-MIMO OFDMA CROSS LAYER RESOURCE ALLOCATION ALGORITHM

We define the following which will be used in the proposed algorithm:

Definition II:
a) Let $A_k^{(i)}$ denote the set of subcarriers allocated to user k at the i-th iteration.
b) Let $\rho_m^{(i)}$ and $\rho_m^{(i)'}$ denote two users assigned to subcarrier m at the i-th iteration. They share the same subcarrier m via MU-MIMO.
c) Let Ω denotes the set of users who may improve average PSNR by gaining a subcarrier.

The propose MU-MIMO OFDMA cross layer algorithm has three steps. First, we assume two antennas at the BS. In the end of this section, we describe the extension to the case of q antennas at the BS

Step (1) Initialization: Let $\Omega = \{1,2,\ldots,K\}$. We initialize $\rho_m^{(0)}$ and $\rho_m^{(0)'}$ as the user pair minimize the noise enhancement on subcarrier m and is given by

$$(\rho_m^{(0)},\rho_m^{(0)'}) = argmin_{(k,l)\in\Omega,k\neq l}\left\{z_{k,l,m}+z_{l,k,m}\right\}. \qquad (13)$$

In [18], every subcarrier is assigned to the user with the best channel response and there is no user grouping due to no MU-MIMO.

Step (2) Water Filling and Application Layer Weighting Calculation: The water filling is used for power allocation. The difference of the power water filling allocation between [18] and proposed method has the noise enhancement factor $z_{k,m}$ due to ZF MU-MIMO receiver and the equivalent channel response for user k on subcarrier m, $\left|H_{k,m}\right|^2 = \frac{1}{2}\sum_{n=1}^{2}\left|H_{k,m}^n\right|^2$, due to two receive antenna at the BS. The power allocation of user k is given by

$$P_{k,m}^* = \left[\frac{1}{\lambda_k}-\frac{1}{\eta\left|H_{k,m}\right|^2/z_{k,m}}\right]^+,\quad \forall m\in A_k^{(i)}, \qquad (14)$$

where $\sum_{m\in A_k^{(i)}}P_{k,m}\leq P$. Note that $P_{k,m}$ may be zero even if subcarrier m is assigned to user k. This can happen when SNR is low and/or there are too many subcarriers for user k such that power waterfilling cannot pass the threshold $\frac{1}{\eta\left|H_{k,m}\right|^2/z_{k,m}}$ (similar to 1/SNR). In this case, subcarrier m has only one

user and is not in MU-MIMO mode anymore. Assume r_k^* is the optimal information rate of user k, and expressed as

$$r_k^* = \sum_{m \in A_k^{(i)}} dw * log_2[1 + \eta P_{k,m}^* \overline{|H_{k,m}|^2}/z_{k,m}] \quad (15)$$

The application layer weighting for user k is given in (11)

$$APP_k = \frac{b_k}{(r_{k+}c_k)^2 MSE_k}$$

b_k and c_k are video-dependent parameters in the application layer. Then select user k^*

$$k^* = argmax_{k \in \Omega} \{APP_k\} \quad (16)$$

for minimum product of MSE distortion, which directly minimize the average PSNR.

For comparison,

$$k^* = argmax_{k \in \Omega} \left\{ \frac{b_k}{(r_{k+}c_k)^2} \right\} \quad (17)$$

for minimum sum of MSE distortion in [18].

Step (3) Subcarrier Reassignment/User Re-Grouping: Consider each subcarrier m not currently allocated to the user k^*. We calculate the old MSE product of all users $\Delta_{\rho_m^{(i)},\rho_m^{(i)'},m}$ where users $\rho_m^{(i)}$ and $\rho_m^{(i)'}$ co-located on subcarrier m. Then we compute the two new MSE products of all users $\Delta_{k^*,\rho_m^{(i)'},m}$ and $\Delta_{\rho_m^{(i)},k^*,m}$ where user k^* replaces either user $\rho_m^{(i)}$ or $\rho_m^{(i)'}$ on subcarrier m.

Note also that where the user k^* replaces either user $\rho_m^{(i)}$ or $\rho_m^{(i)'}$ on subcarrier m, the noise power enhancement factor after zero-forcing MU-MIMO detector also changes. For comparison, [18] does not considers MU-MIMO, only one new MSE is computed, and the noise power does not change after subcarrier reassignment.

We find subcarrier m^* whose product of users' MSE decreases most due to subcarrier reassignment,

$$m^* = argmax_{m \in \{1,...,M\} \backslash A_{k^*}^{(i)}} \left\{ \Delta_{\rho_m^{(i)},\rho_m^{(i)'},m} - min \left\{ \Delta_{k^*,\rho_m^{(i)'},m}, \Delta_{\rho_m^{(i)},k^*,m} \right\} \right\}$$

If

$$\Delta_{\rho_{m^*}^{(i)},\rho_{m^*'}^{(i)},m^*} - min \left\{ \Delta_{k^*,\rho_{m^*'}^{(i)},m^*}, \Delta_{\rho_{m^*}^{(i)},k^*,m^*} \right\} > 0,$$

we perform subcarrier reassignment because the product of users' MSE will decrease (average PSNR increase). There are two cases because there are two users on subcarrier m^*

a) If $\Delta_{k^*,\rho_{m^*'}^{(i)},m^*} < \Delta_{\rho_{m^*}^{(i)},k^*,m^*}$, user k^* replaces user $\rho_{m^*}^{(i)}$ on subcarrier m at iteration $i+1$, $\rho_{m^*}^{(i+1)} = k^*$ and go back to step (2)

b) If $\Delta_{\rho_{m^*}^{(i)},k^*,m^*} < \Delta_{k^*,\rho_{m^*'}^{(i)},m^*}$ user k^* replaces user $\rho_{m^*'}^{(i)}$ on subcarrier m at iteration $i+1$, $\rho_{m^*'}^{(i+1)} = k^*$ and go back to Step (2).

TABLE 1. The simulation parameters.

Parameter	Value
K (the number of users)	4/8/12
SER_t (the target symbol error rate)	0.1
γ (the path-loss exponent)	2.4
channel code	Convolutional code with code rate u =1/2
Video frame rate	30 frames/s
video compression	H.264/AVC reference software JM11.0 [32]
Group of Pictures (GOP) size	15 frames (I-P-P-P)
frame size	10 slices
error concealment	slice copy

If

$$\Delta_{\rho_{m^*}^{(i)},\rho_{m^*'}^{(i)},m^*} - min \left\{ \Delta_{k^*,\rho_{m^*'}^{(i)},m^*}, \Delta_{\rho_{m^*}^{(i)},k^*,m^*} \right\} < 0,$$

the overall video quality (product of MSE of all users) will not improve if user k^* gain any subcarrier, so we update $\Omega = \Omega \backslash k^*$. In other words, user k^* will not have a chance to gain a subcarrier.

Then, $i = i + 1$, and return to step (2) to update k^*.

For example, the subcarrier 8 has been assigned to the user 1 and the user 3, the user 4 with the largest APP_i in (11). We first calculate MSE product $\Delta_{1,3,8}$ of all users. There are two cases: assign the subcarrier to the user 1 and the user 4 or assign the subcarrier to user 4 and user 3. We calculate both MSE products $\Delta_{1,4,8}$ and $\Delta_{4,3,8}$ and find $min(\Delta_{1,4,8}, \Delta_{4,3,8})$. If $\Delta_{1,3,8} - min\left(\Delta_{1,4,8}, \Delta_{4,3,8}\right) < 0$, we don't reassign subcarrier 8 because the MSE product does not decrease. Otherwise subcarrier 8 is reassigned to user 4. Specifically, user 4 replaces user 3 on subcarrier 8 if $min\left(\Delta_{1,4,8}, \Delta_{4,3,8}\right) = \Delta_{1,4,8}$; user 4 replaces the user 1 at subcarrier 8 if $min\left(\Delta_{1,4,8}, \Delta_{4,3,8}\right) = \Delta_{4,3,8}$.

Although we assume two antennas at the BS above, the proposed cross-layer resource allocation algorithm is easily extended to arbitrary number of antennas, q, at the BS. Specifically, in step (1), C_q^K grouping cases are considered on each subcarrier, instead of $C_2^K = K(K-1)/2$ cases are considered for two antennas at the BS. In step (3), subcarrier reassignment would consider q cases instead of two cases.

V. NUMERICAL RESULT

The uplink OFDMA system has two receive antenna and 16 subcarriers, each of this subcarrier with $dw = $ 50kHz bandwidth, and the adaptive modulation alphabet of M-QAM, M = 4, . . . , 256. The other parameters are given in Table 1. These parameters are the same as [18].

The distance is assumed uniformly distributed between 20m and 60m. For cross layer resource allocation, it is highly unlikely for the nearest user to monopolize the subcarriers
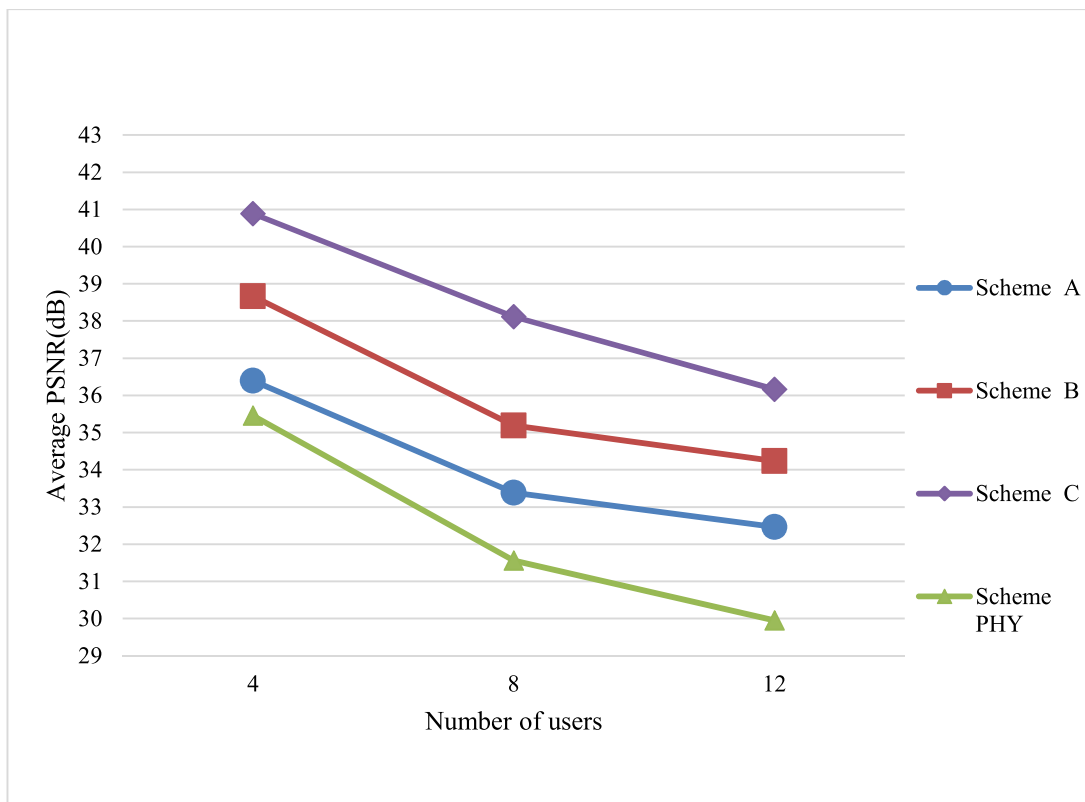
FIGURE 3. Average PSNR (video quality) vs. number of users, 16 subcarriers, SNR = 15dB.
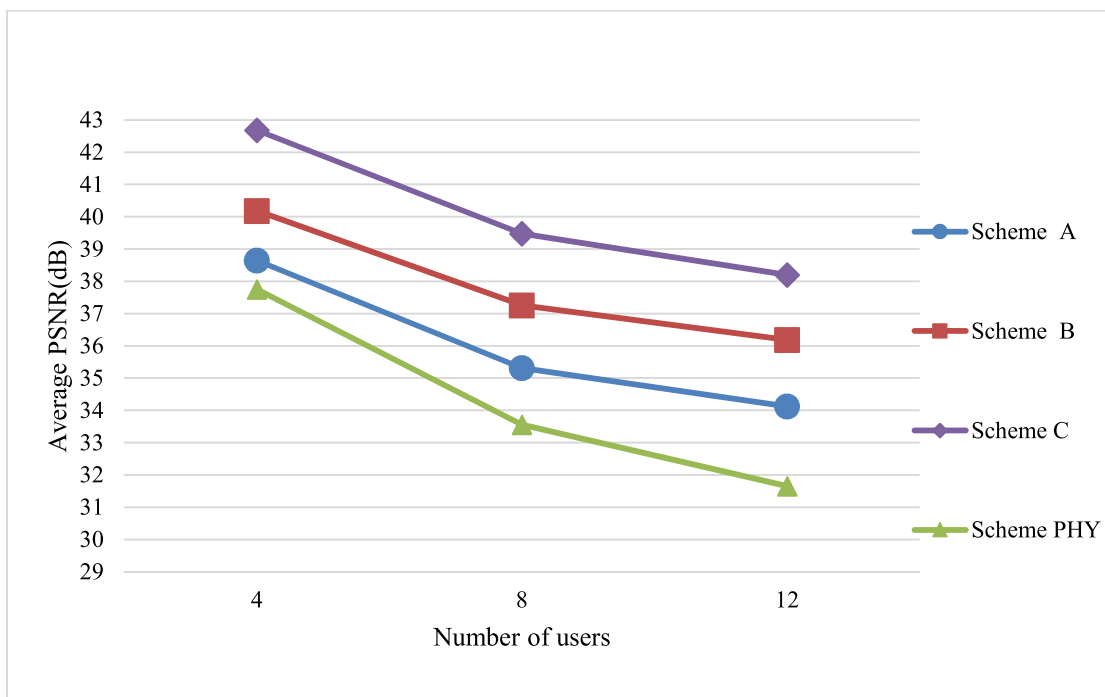

FIGURE 4. Average PSNR (video quality) vs. number of users, 16 subcarriers, SNR = 18dB.

because of step (3) in Sec. IV, which considers RD information in the application layer. Assume the nearest user, say user i, has most subcarriers in step (1), where only physical

layer CSI information is used. Its $APPi$ in (11) will be very small (note that $(r_i + c_i)^2$ is very large if r_i is large). Almost all the other users are eligible to take away user i's subcarriers
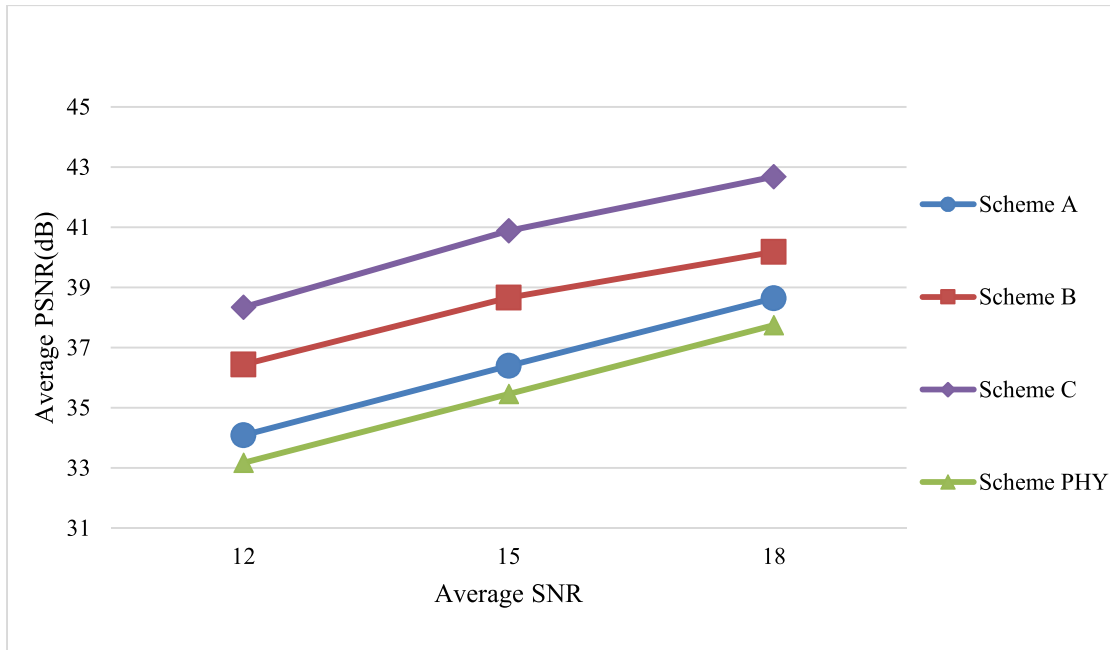
FIGURE 5. Average PSNR (video quality) vs. Average SNR, 16 subcarriers, 4 users.

because we give the user j with largest $APPj$ priority to take away other users' subcarrier and increased average PSNR. Thus user i would lose many subcarriers in step (3).

For comparison purpose (Schemes A and B defined below), the same as [18], we assume that one GOP is transmitted in one time slot where the channel is constant, but independent from slot to slot. The cross layer resource allocation is conducted once per GOP/slot. The GOP length can be shorter, so the slot duration can be shorter too. The simulation result is the average of five hundred times for each user. Average SNR is defined similar to that [18] as follows. First, $\overline{\left|H_{k,m}\right|^2} = \frac{1}{2}\sum_{n=1}^{2}\left|H_{k,m}^n\right|^2$ is the equivalent channel response for user k on subcarrier m. Then each user's SNR is obtained by averaging over the subcarriers each user allocated. Finally average SNR is obtained by averaging over each user' SNR. We adjust the noise power spectral density according to five hundred runs (transmitted power and channel vary five hundred times) such that average SNR is the set value (e.g. 15dB).

The video MSE distortion model in (4) and (6) is the same as that of [18], which adopts the empirical model in [31] for simplicity and accuracy. The video encoder rates are 80, 100, 120, 140, 160, 180, 200, 220, 240, 280, 300, 340, 380, 420, 460, 500 and 600 kbps. The operational points are used to fit the RD function by nonlinear regression. The multiuser diversity in the application layer is created by assigning random starting points of the same video to different users. Instead of RD function $MSE_k = a_k + \frac{\omega_k}{B_k + \upsilon_k}$ in (4), we use RD function $MSE_k = a_k + \frac{b_k}{R + c_k}$ in (6), which incorporates channel code rate, time slot length and OFDM symbol duration. We use the same sequence of CIF video as [18]. It is a travel documentary

with both low and high motion of GOPs. The value range of the parameters is as follows: $a_k = -8 \sim -11$, $b_k = 7 \times 10^6 \sim 10 \times 10^6$, $c_k = -0.8 \times 10^3 \sim -9.5 \times 10^3$. These parameters are specific for a given video sequence and video codec. For high-complexity video like fast motion one, b_k is relative large [18]. These parameters can't be derived from common signal statistics like variance, correlation etc. because it is an empirical model [31].

We consider the following schemes:

Scheme PHY: ZF-SVD MU-MIMO detector scheme in [29]. Its resource allocation considers physical layer only.

Scheme A: the non-MU-MIMO scheme in [18] whose optimization objective is minimization of sum of users' video MSE distortion.

Scheme B: the non-MU-MIMO scheme in [18] but optimization objective function is proposed maximization of average of users' PSNR.

Scheme C: proposed MU-MIMO scheme. The optimization objective function is proposed maximization of average of users' PSNR.

In all schemes (non-MU-MIMO and MU-MIMO), we assume each user has the same power constraint 0.1(W), so the total power constraint of all users is also the same. Note that each user in Scheme C has more assigned subcarriers due to MU-MIMO, so its power is splitting more thinly into more subcarriers.

The simulation results for SNR = 15dB and 18dB are shown in Fig. 3 and Fig. 4, respectively. The average PSNR of Scheme B outperforms that of Scheme A by about 2dB in 4, 8, 12-use cases. It clearly shows the PSNR gain if we directly optimize the average PSNR instead of the sum

Scheme C

Scheme B

Scheme A

Scheme PHY

FIGURE 6. Comparison of visual results, in terms of received images (of H.264/AVC video(s)), between Schemes C, B, A and PHY, 4 users, SNR = 15dB.

Scheme C

Scheme B

Scheme A

Scheme PHY

FIGURE 7. Zoom of the right-bottom corner of Fig. 6.

of users' video MSE distortion, the novelty and contribution 1) of this paper in Introduction section. The average PSNR of Scheme C outperforms that of Scheme B by about 2dB in 4, 8, 12-users. The MU-MIMO give additional PSNR gain because two users shares the same resource, the novelty and contribution 2) of this paper in Introduction section. We also note that when the number of users increase, the average

number of subcarriers each user can get decreases, information rate decreases, MSE increases, and thus the average SNR decreases. Compared to the scheme in [18] (Scheme A), the proposed scheme (Scheme C) has about 4dB gain in average PSNR. Scheme PHY (physical layer only resource allocation) has worse PSNR than other cross layer resource

allocation schemes (Scheme A,B,C) especially when there are more users because the physical/application cross layer resource allocation algorithm exploits the application layer diversity where different users have different RD tradeoff but the physical layer only resource allocation cannot.

In Fig. 5, the video quality for various SNR is shown. The proposed MU-MIMO OFDMA cross layer resource allocation (Scheme C) offer 1.9, 2.2, 2.5dB PSNR gain over non-MU-MIMO scheme (Scheme B) for the SNR = 12, 15, 18dB, respectively. The PSNR gain of MU-MIMO increases as SNR increases because it is more likely that all subcarriers are in MU-MIMO modes. As stated in step (2) of Sec. IV, the assigned power $P_{k,m}$ is less likely to be zero (MU-MIMO mode degenerates to non-MU-MIMO mode on subcarrier m) because power waterfilling can more easily pass the threshold $\frac{1}{\eta |H_{k,m}|^2/z_{k,m}}$ (similar to 1/SNR).

In Figs. 6 and 7, we add comparison of visual results, in terms of received images (of H.264/AVC video(s)), between Schemes C, B, A and PHY. We observe that, from the top to the bottom, the clarity and color saturation decrease. This confirms the PSNR results: Scheme C > Scheme B > Scheme A > Scheme PHY.

The complexity analysis of Schemes C, B, A, PHY is as follows. The proposed algorithm (Scheme C) has the following complexity. In step (1), every possible user pair is checked on each subcarrier, and thus the complexity is $O(M * K(K-1)/2)$. At every iteration, the user k with the largest APP_k tests all M subcarriers (two users in one subcarrier) for opportunity of the subcarrier reallocation, so the complexity is $O(2M)$. Let L be the iteration times among steps (2) and (3). The total complexity is $O(M * K(K-1)/2 + 2M * L)$. The complexity of Scheme B and A is both $O(M * K + M * L)$ because there is no MU-MIMO grouping like Scheme C. The complexity of Scheme PHY is $O(M * K)$ because there is no cross layer iterative subcarrier reassignment.

VI. CONCLUSION
We propose average PSNR optimized resource allocation crossing physical and application layers for MU-MIMO uplink OFDMA video transmission systems. We derive the new optimal condition for the average PSNR optimized cross layer resource allocation because the previous scheme [18] optimizes the total video distortion and does not consider MU-MIMO. The simulation results show about 4dB gain in PSNR over cross layer scheme [18] and 5dB gain in PSNR over physical layer only scheme [29] for 2- receive-antenna BS, 4 users, and SNR range 12-18 dB.

APPENDIX A
PROOF OF THEOREM I
Unlike minimization of sum of MSE distortion in [18], the optimization problem in this paper considers maximization of average PSNR, which is equivalent to minimization of product of MSE distortion. Additional difference is the noise enhancement factor z_i due to ZF MU-MIMO receiver.

Assume B_1^{opt} and B_2^{opt} are the optimal band assignment, and assume $B_1^{opt} \cup \theta$ and $B_2^{opt} - \theta$ are the new band assignment. If a band assignment is optimal, any reassignment would have a smaller or equal product of MSE, and then

$$MSE_1 * MSE_2 \leq MSE_1' * MSE_2' \qquad (A.1)$$

where MSE_1, MSE_2 is the MSE for user 1 (rate r_1) and 2 (rate r_2), respectively before band reassignment; MSE_1', MSE_2' is the MSE for user 1 (rate $r_1 + \Delta r_1$) and 2 (rate $r_2 - \Delta r_2$) respectively after band reassignment. Here Δr_1 and Δr_2 are the change of the information rate due to band reassignment.

Then applying video MSE model into (A.1), we have

$$\left(a_1 + \frac{b_1}{r_1 + c_1} \right) \left(a_2 + \frac{b_2}{r_2 + c_2} \right)$$
$$\leq \left(a_1 + \frac{b_1}{(r_1 + \Delta r_1) + c_1} \right) \left(a_2 + \frac{b_2}{(r_2 - \Delta r_2) + c_2} \right) \qquad (A.2)$$

Reorganizing (A.2), we get

$$\frac{a_2 b_1}{r_1 + c_1} + \frac{a_1 b_2}{r_2 + c_2} + \frac{b_1 b_2}{(r_1 + c_1)(r_2 + c_2)}$$
$$\leq \frac{a_2 b_1}{r_1 + \Delta r_1 + c_1} + \frac{a_1 b_2}{r_2 - \Delta r_2 + c_2}$$
$$+ \frac{b_1 b_2}{(r_1 + \Delta r_1 + c_1)(r_2 - \Delta r_2 + c_2)} \qquad (A.3)$$

Combining terms, we get (A.4), as shown at the top of the next page and, Reorganizing (A.4), we get (A.5), as shown at the top of the next page,

Note that $1 + \Delta r_1/(r_1 + c_1) \approx 1$, $1 - \Delta r_2/(r_2 + c_2) \approx 1$, and $\frac{\Delta r_1 \Delta r_2}{(r_1+c_1)^2(r_2+c_2)^2} \approx 0$, and we have

$$\left[\frac{a_2 b_1}{(r_1 + c_1)^2} + \frac{b_1 b_2}{(r_2 + c_2)(r_1 + c_1)^2} \right] \Delta r_1$$
$$\leq \left[\frac{a_1 b_2}{(r_2 + c_2)^2} + \frac{b_1 b_2}{(r_1 + c_1)(r_2 + c_2)^2} \right] \Delta r_2 \qquad (A.6)$$

Reorganizing (A.6), and we have

$$\frac{b_1}{(r_1 + c_1)^2} \left(a_2 + \frac{b_2}{r_2 + c_2} \right) \Delta r_1$$
$$\leq \frac{b_2}{(r_2 + c_2)^2} \left(a_1 + \frac{b_1}{r_1 + c_1} \right) \Delta r_2 \qquad (A.7)$$

and

$$\frac{b_1 * MSE_2}{(r_1 + c_1)^2} \Delta r_1 \leq \frac{b_2 * MSE_1}{(r_2 + c_2)^2} \Delta r_2 \qquad (A.8)$$

We divide both sides by $MSE_1 * MSE_2$, and get

$$\frac{b_1}{MSE_1 * (r_1 + c_1)^2} \Delta r_1 \leq \frac{b_2}{MSE_2 * (r_2 + c_2)^2} \Delta r_2 \qquad (A.9)$$

where $\frac{b_i}{MSE_i(r_i+c_i)^2}$ is the fifth layer term, and Δr_i is first layer term.

$$\frac{a_2 b_1 \Delta r_1}{(r_1 + c_1)^2 + \Delta r_1 (r_1 + c_1)} - \frac{a_1 b_2 \Delta r_2}{(r_2 + c_2)^2 - \Delta r_2 (r_2 + c_2)} + \frac{b_1 b_2 \left[(r_1 + \Delta r_1 + c_1)(r_2 - \Delta r_2 + c_2) - (r_1 + c_1)(r_2 + c_2) \right]}{\left[(r_1 + c_1)^2 + \Delta r_1 (r_1 + c_1) \right] \left[(r_2 + c_2)^2 - \Delta r_2 (r_2 + c_2) \right]} \leq 0$$

$$\frac{a_2 b_1 \Delta r_1}{(r_1 + c_1)^2 + \Delta r_1 (r_1 + c_1)} - \frac{a_1 b_2 \Delta r_2}{(r_2 + c_2)^2 - \Delta r_2 (r_2 + c_2)} + \frac{b_1 b_2 \left[\Delta r_1 (r_2 + c_2) - \Delta r_2 (r_1 + c_1) - \Delta r_1 \Delta r_2 \right]}{\left[(r_1 + c_1)^2 + \Delta r_1 (r_1 + c_1) \right] \left[(r_2 + c_2)^2 - \Delta r_2 (r_2 + c_2) \right]} \leq 0 \tag{A.4}$$

$$\frac{a_2 b_1 \Delta r_1 / (r_1 + c_1)^2}{1 + \Delta r_1 / (r_1 + c_1)} - \frac{a_1 b_2 \Delta r_2 / (r_2 + c_2)^2}{1 - \Delta r_2 / (r_2 + c_2)} + \frac{b_1 b_2 \left[\frac{\Delta r_1}{(r_2+c_2)(r_1+c_1)^2} - \frac{\Delta r_2}{(r_1+c_1)(r_2+c_2)^2} - \frac{\Delta r_1 \Delta r_2}{(r_1+c_1)^2(r_2+c_2)^2} \right]}{\left[1 + \Delta r_1 / (r_1 + c_1) \right] \left[1 - \Delta r_2 / (r_2 + c_2) \right]} \leq 0 \tag{A.5}$$

Then we are going to find $\frac{\Delta r_1}{\Delta r_2}$ in the new band assignment. $P_{1,\theta}$ is the total power the 1st user will put over band θ after the reallocation. Before reallocation, the 1st user' water-filling level is $W_1 = P_1(f) + \frac{1}{\eta |H_1(f)|^2 / z_1}$. After reallocation, we uniformly reduce $P_{1,\theta}$ over B_1^{opt}, the water level over band B_1^{opt} is reduced by $\frac{P_{1,\theta}}{|B_1^{opt}|}$, and the water level over B_1^{opt} become $W_1' = W_1 - \frac{P_{1,\theta}}{|B_1^{opt}|}$.

And we reassign $P_{1,\theta}$ uniformly over band θ. the water level over band θ is increased by $\varphi_1^\theta = P_{1,\theta} / |\theta|$ and the water level over θ, W_1', become

$$\frac{1}{\eta |H_1^\theta|^2} + \frac{P_{1,\theta}}{|\theta|} = W_1 - \frac{P_{1,\theta}}{|B_1^{opt}|} \tag{A.10}$$

where $H_1^\theta = H_1 \left(f_0 + \frac{|\theta|}{2} \right)$ is the channel coefficient of the band θ, and f_0 is the band θ's left limit.

We solve $P_{1,\theta}$ in (A.10) and obtain

$$P_{1,\theta} = \left(\frac{\left| B_1^{opt} \right| |\theta|}{|\theta| + \left| B_1^{opt} \right|} \right) \left(W_1 - \frac{1}{\eta |H_1^\theta|^2} \right) \tag{A.11}$$

if $|\theta| \to 0$

$$P_{1,\theta} = \left(\frac{\left| B_1^{opt} \right| |\theta|}{|\theta| + \left| B_1^{opt} \right|} \right) \varphi_1^\theta \cong |\theta| \varphi_1^\theta \tag{A.12}$$

The user 1's old rate is

$$\int_{B_1^{opt}} \log_2 \left(1 + \eta P_1(f) |H_1(f)|^2 / z_1 \right) df \, ;$$

after gaining θ, the new rate is given by

$$\left(\int_{B_1^{opt}} \log_2 \left(1 + \eta \left(P_1(f) - \frac{P_{1,\theta}}{\left| B_1^{opt} \right|} \right) |H_1(f)|^2 / z_1 \right) df \right.$$

$$\left. + |\theta| \log_2 \left(1 + \eta \frac{P_{1,\theta}}{|\theta|} |H_1^\theta|^2 \right) \right) \tag{A.13}$$

The difference in rate is

$$\Delta r_1 = \int_{B_1^{opt}} \log_2 \left(\frac{1 + \eta \left(P_1(f) - \frac{P_{1,\theta}}{\left| B_1^{opt} \right|} \right) |H_1(f)|^2 / z_1}{\left(1 + \eta P_1(f) |H_1(f)|^2 / z_1 \right)} \right) df$$

$$+ |\theta| \log_2 \left(1 + \eta \frac{P_{1,\theta}}{|\theta|} |H_1^\theta|^2 \right) \tag{A.14}$$

In a similar way

$$P_{2,\theta} \cong \varphi_2^\theta |\theta| \text{ if } |\theta| \to 0 \tag{A.15}$$
$$\varphi_2^\theta = P_{2,\theta} / |\theta|$$

$$\Delta r_2 = |\theta| \log_2 \left(1 + \eta \frac{P_{2,\theta}}{|\theta|} |H_2^\theta|^2 / z_2 \right)$$

$$- \int_{B_2^{opt}} \log_2 \left(1 + \frac{\eta P_{2,\theta} |H_2(f)|^2}{\left| B_2^{opt} \right| \left(1 + \eta P_2(f) |H_2(f)|^2 / z_2 \right)} \right) \tag{A.16}$$

We take limit as $|\theta| \to 0$, (A.17) as shown at the top of the next page.

Note that

$$\lim_{|\theta| \to 0} \frac{d}{d\theta} \ln \left(1 - \frac{\eta \phi_1^\theta |\theta| |H_1(f)|^2}{\left| B_1^{opt} \right| \left(1 + \eta P_1(f) |H_1(f)|^2 \right)} \right)$$

$$= - \frac{\eta \phi_1^\theta |H_1(f)|^2}{\left| B_1^{opt} \right| \left(1 + \eta P_1(f) |H_1(f)|^2 \right)} \tag{A.18}$$

By L'Hopital's rule,

$$\lim_{|\theta| \to 0} \frac{\Delta r_1}{\Delta r_2}$$

$$= \frac{\ln \left(1 + \eta \phi_1^\theta |H_1^\theta|^2 \right) - \int_{B_1^{opt}} \frac{\eta |H_1(f)|^2 / z_1}{\left| B_1^{opt} \right| (1 + \eta P_1(f) |H_1(f)|^2 / z_1)} \phi_1^\theta df}{\ln \left(1 + \eta \phi_2^\theta |H_2^\theta|^2 \right) - \int_{B_2^{opt}} \frac{\eta |H_2(f)|^2 / z_2}{\left| B_2^{opt} \right| (1 + \eta P_2(f) |H_2(f)|^2 / z_2)} \phi_2^\theta df} \tag{A.19}$$

We take (A.9) and (A.19) together, and the optimal assignment satisfies This completes the proof of **Theorem I**, (A.20), as shown at the top of the next page.

$$\lim_{|\theta|\to 0}\frac{\Delta r_1}{\Delta r_2} = \lim_{|\theta|\to 0}\frac{\int_{B_1^{opt}} \ln\left(1-\frac{\eta\phi_1^\theta|\theta||H_1(f)|^2}{\left|B_1^{opt}\right|\left(1+\eta P_1(f)|H_1(f)|^2\right)}\right)df + |\theta|\ln\left(1+\eta\phi_1^\theta\left|H_1^\theta\right|^2\right)}{|\theta|\ln\left(1+\eta\phi_2^\theta\left|H_2^\theta\right|^2\right) - \int_{B_2^{opt}} \ln\left(1+\frac{\eta\phi_2^\theta|\theta||H_2(f)|^2}{\left|B_2^{opt}\right|\left(1+\eta P_2(f)|H_2(f)|^2\right)}\right)df} \tag{A.17}$$

$$\frac{\frac{b_1}{MSE_1(r_1+c_1)^2}\left\{\ln\left(1+\eta\phi_1^\theta\left|H_1^\theta\right|^2\right) - \int_{B_1^{opt}}\frac{\eta|H_1(f)|^2/z_1}{\left|B_1^{opt}\right|(1+\eta P_1(f)|H_1(f)|^2/z_1)}\phi_1^\theta df\right\}}{\frac{b_2}{MSE_2(r_2+c_2)^2}\left\{\ln\left(1+\eta\phi_2^\theta\left|H_2^\theta\right|^2\right) - \int_{B_2^{opt}}\frac{\eta|H_2(f)|^2/z_2}{\left|B_2^{opt}\right|(1+\eta P_2(f)|H_2(f)|^2/z_2)}\phi_2^\theta df\right\}} \le 1 \tag{A.20}$$

$$\frac{\frac{b_i}{MSE_i(r_i+c_i)^2}\left\{\ln\left(1+\eta\phi_i^\theta\left|H_i^\theta\right|^2\right) - \int_{B_i^{opt}}\frac{\eta|H_i(f)|^2/z_i}{\left|B_i^{opt}\right|(1+\eta P_i(f)|H_i(f)|^2/z_i)}\phi_i^\theta df\right\}}{\frac{b_j}{MSE_j(r_j+c_j)^2}\left\{\ln\left(1+\eta\phi_j^\theta\left|H_j^\theta\right|^2\right) - \int_{B_j^{opt}}\frac{\eta|H_j(f)|^2/z_j}{\left|B_j^{opt}\right|(1+\eta P_j(f)|H_j(f)|^2/z_j)}\phi_j^\theta df\right\}} \le 1 \tag{A.21}$$

For more than two users, we deduce that, for a band θ to be reallocated from user i to user j, the below relation must be met for any user $i \neq j$, (A.21), as shown at the top of the this page.

ACKNOWLEDGMENT
The authors would like to thank former MS. Students Mr. Hao-Sheng Suo and Mr. Wen-Da Tsai for producing simulation figures.

REFERENCES
[1] C.-P. Li, S.-H. Wang, and K.-C. Chan, "Low complexity transmitter architectures for SFBC MIMO-OFDM systems," *IEEE Trans. Commun.*, vol. 60, no. 6, pp. 1712–1718, Jun. 2012.

[2] W.-C. Huang, Y.-S. Yang, and C.-P. Li, "A new pilot architecture for sub-band uplink OFDMA systems," *IEEE Trans. Broadcast.*, vol. 59, no. 3, pp. 461–470, Sep. 2013.

[3] K.-C. Lee, S.-H. Wang, C.-P. Li, H.-H. Chang, and H.-J. Li, "Adaptive resource allocation algorithm based on cross-entropy method for OFDMA systems," *IEEE Trans. Broadcast.*, vol. 60, no. 3, pp. 524–531, Sep. 2014.

[4] J.-J. Chen, S.-L. Wu, and W.-Y. Lin, "A cross-layer design for energy efficient sleep scheduling in uplink transmissions of IEEE 802.16 broadband wireless networks," in *Advances in Intelligent Systems and Applications*, vol. 1. Berlin, Germany: Springer, 2013, pp. 635–644.

[5] S.-M. Tseng, "An iterative ICI cancellation and decoding scheme for coded OFDM systems in mobile channels," *IEICE Trans. Fundam. Electron., Commun. Comput. Sci.*, vol. E88-A, no. 11, pp. 3085–3091, Nov. 2005.

[6] *Evolved Universal Terrestrial Radio Access (E-UTRA); Physical Layer Procedures*, document TS 36.213, 3rd Generation Partnership Project (3GPP), France, Sep. 2008. [Online]. Available: http://www.3gpp.org/ftp/Specs/html-info/36213.htm

[7] I. C. Wong and B. L. Evans, "Optimal resource allocation in the OFDMA downlink with imperfect channel knowledge," *IEEE Trans. Commun.*, vol. 57, no. 1, pp. 232–241, Jan. 2009.

[8] Z. Wang, L. Liu, X. Wang, and J. Zhang, "Resource allocation in OFDMA networks with imperfect channel state information," *IEEE Commun. Lett.*, vol. 18, no. 9, pp. 1611–1614, Sep. 2014.

[9] M.-L. Tham, C.-O. Chow, Y.-H. Xu, and N. Ramli, "Two-level scheduling for video transmission over downlink OFDMA networks," *PLoS ONE*, vol. 11, no. 2, p. e0148625, Feb. 2016.

[10] G. W. Cook, J. Prades-Nebot, Y. Liu, and E. J. Delp, "Rate-distortion analysis of motion-compensated rate scalable video," *IEEE Trans. Image Process.*, vol. 15, no. 8, pp. 2170–2190, Aug. 2006.

[11] Z. Chen and K. N. Ngan, "Recent advances in rate control for video coding," *Signal Process., Image Commun.*, vol. 22, no. 1, pp. 19–38, 2007.

[12] M. Tiwari, T. Groves, and P. C. Cosman, "Competitive equilibrium bitrate allocation for multiple video streams," *IEEE Trans. Image Process.*, vol. 19, no. 4, pp. 1009–1021, Apr. 2010.

[13] S.-L. Wu and W.-W. Wang, "Energy-efficient multimedia multicast scheduling and resource allocation algorithms for OFDMA-based systems," in *Proc. CIT/IUCC/DASC/PICom*, Liverpool, U.K., Oct. 2015, pp. 1377–1382.

[14] G.-M. Su, Z. Han, M. Wu, and K. J. R. Liu, "A scalable multiuser framework for video over OFDM networks: Fairness and efficiency," *IEEE Trans. Circuits Syst. Video Technol.*, vol. 16, no. 10, pp. 1217–1231, Oct. 2006.

[15] S. Cicalo and V. Tralli, "Distortion-fair cross-layer resource allocation for scalable video transmission in OFDMA wireless networks," *IEEE Trans. Multimedia*, vol. 16, no. 3, pp. 848–863, Apr. 2014.

[16] K. Lin and S. Dumitrescu, "Cross-layer resource allocation for scalable video over OFDMA wireless networks: Tradeoff between quality fairness and efficiency," *IEEE Trans. Multimedia*, vol. 19, no. 7, pp. 1654–1669, Jul. 2017.

[17] D. Liu, H. Cui, J. Wu, and C. Luo, "Resource allocation for uncoded multiuser video transmission over wireless networks," *Mobile Netw. Appl.*, vol. 21, no. 6, pp. 950–961, Dec. 2016.

[18] D. Wang, L. Toni, P. C. Cosman, and L. B. Milstein, "Uplink resource management for multiuser OFDM video transmission systems: Analysis and algorithm design," *IEEE Trans. Commun.*, vol. 61, no. 5, pp. 2060–2073, May 2013.

[19] Y.-F. Chen, S.-M. Tseng, C.-H. Shen, and M.-S. He, "Cross layer 1, 2 and 5 resource allocation in uplink turbo-coded HARQ based OFDMA video transmission systems," *Wireless Pers. Commun.*, vol. 98, no. 2, pp. 1997–2008, Feb. 2018.

[20] S.-M. Tseng, Y.-F. Chen, P.-H. Chiu, and H.-C. Chi, "Jamming resilient cross-layer resource allocation in uplink HARQ-based SIMO OFDMA video transmission systems," *IEEE Access*, vol. 5, pp. 24908–24919, 2017.

[21] Y.-S. Yang, J.-W. Pu, P.-H. Yeh, C.-P. Li, and H.-J. Li, "Investigation on distributed user selection for uplink multicell systems with MIMO," in *Proc. IEEE 81st Veh. Technol. Conf. (VTC Spring)*, Glasgow, U.K., May 2015, pp. 1–5.

[22] E. Castañeda, A. Silva, A. Gameiro, and M. Kountouris, "An overview on resource allocation techniques for multi-user MIMO systems," *IEEE Commun. Surveys Tuts.*, vol. 19, no. 1, pp. 239–284, 1st Quart., 2017.

[23] G. Femenias, F. Riera-Palou, and J. Pastor, "Resource allocation in block diagonalization-based multiuser MIMO-OFDMA networks," in *Proc. 11th Int. Symp. Wireless Commun. Syst. (ISWCS)*, Aug. 2014, pp. 411–417.

[24] G. Femenias and F. Riera-Palou, "Scheduling and resource allocation in downlink multiuser MIMO-OFDMA systems," *IEEE Trans. Commun.*, vol. 64, no. 5, pp. 2019–2034, May 2016.

[25] Y. Mao and V. O. K. Li, "Cluster-based resource allocation with adaptive CoMP in multi-cell MU-MIMO OFDMA system," in *Proc. IEEE Int. Conf. Signal Process., Commun. Comput. (ICSPCC)*, Hong Kong, Aug. 2016, pp. 1–6.

[26] Y. Sakata, T. Murakami, Y. Takatori, M. Mizoguchi, and F. Maehara, "Simple resource allocation scheme for heterogeneous traffic in MU-MIMO-OFDMA systems," in *Proc. Asia–Pacific Conf. Commun. (APCC)*, Pattaya, Thailand, Oct. 2014, pp. 189–193.

[27] X. Lu, Q. Ni, W. Li, and H. Zhang, "Dynamic user grouping and joint resource allocation with multi-cell cooperation for uplink virtual MIMO systems," *IEEE Trans. Wireless Commun.*, vol. 16, no. 6, pp. 3854–3869, Jun. 2017.

[28] A. Grassi, G. Piro, G. Bacci, and G. Boggia, "Uplink resource management in 5G: When a distributed and energy-efficient solution meets power and QoS constraints," *IEEE Trans. Veh. Technol.*, vol. 66, no. 6, pp. 5176–5189, Jun. 2017.

[29] A. N. Alyahya and J. Ilow, "Zero-forcing assisted spatial stream allocation in multiuser MIMO systems," in *Proc. IEEE 28th Can. Conf. Elect. Comput. Eng.*, Halifax, NS, Canada, May 2015, pp. 1030–1035.

[30] S. Yang and L. Hanzo, "Fifty years of MIMO detection: The road to large-scale MIMOs," *IEEE Commun. Surveys Tuts.*, vol. 17, no. 4, pp. 1941–1988, 4th Quart., 2015.

[31] K. Stuhlmuller, N. Farber, M. Link, and B. Girod, "Analysis of video transmission over lossy channels," *IEEE J. Sel. Areas Commun.*, vol. 18, no. 6, pp. 1012–1032, Jun. 2000.

[32] H. Schwarz, D. Marpe, and T. Wiegand, "Overview of the scalable video coding extension of the H.264/AVC standard," *IEEE Trans. Circuits Syst. Video Technol.*, vol. 17, no. 9, pp. 1103–1120, Sep. 2007.
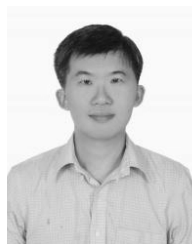
SHU-MING TSENG received the B.S. degree in electrical engineering from National Tsing Hua University, Taiwan, in 1994, and the M.S. and Ph.D. degrees in electrical engineering from Purdue University, West Lafayette, IN, USA, in 1995 and 1999, respectively. From 1999 to 2001, he was with the Department of Electrical Engineering, Chang Gung University, Taiwan. Since 2001, he has been with the Department of Electronic Engineering, National Taipei University of Technology, Taipei, Taiwan, where he has been a Professor since 2007. He is the author of 42 SCI journal papers. His research interests include NOMA, MU-MIMO, OFDMA, cross layer optimization for video transmission, jamming resiliency, network performance evaluation, software defined radio, and optical systems. He has served as an Editor for *KSII Transactions on Internet and Information Systems*, indexed in SCI, since 2013.

YUNG-FANG CHEN received the B.S. degree in computer science and information engineering from National Taiwan University, Taipei, Taiwan, in 1990, the M.S. degree in electrical engineering from the University of Maryland at College Park, College Park, in 1994, and the Ph.D. degree in electrical engineering from Purdue University, West Lafayette, IN, USA, in 1998. From 1998 to 2000, he was with Lucent Technologies, Whippany, NJ, USA, where he was with the CDMA Radio Technology Performance Group. Since 2000, he has been with the faculty of the Department of Communication Engineering, National Central University, Taoyuan, Taiwan, where he is currently a Professor and the Chairman of the Department. His research interests include resource management and signal processing algorithm designs for wireless communication systems.

● ● ●